UvA-DARE (Digital Academic Repository)

Fibrin network adaptation to cell-generated forces

van Esterik, F.A.S.; Vega, A.V.; Pajanonot, K.A.T.; Cuizon, D.R.; Velayo, M.E.; Dejito, J.; Flores, S.L.; Klein-Nulend, J.; Bacabac, R.G.

ORIGINAL CONTRIBUTION

CrossMark

Fibrin network adaptation to cell-generated forces

Fransisca A. S. van Esterik[1,2] · Arianne V. Vega[3] · Kristian A. T. Pajanonot[3] · Daniel R. Cuizon[3] · Michelle E. Velayo[3] · Jahazel Dejito[3] · Stephen L. Flores[3] · Jenneke Klein-Nulend[1] · Rommel G. Bacabac[3]

Abstract

Fibrin promotes wound healing by serving as provisional extracellular matrix for fibroblasts that realign and degrade fibrin fibers, and sense and respond to surrounding substrate in a mechanical-feedback loop. We aimed to study mechanical adaptation of fibrin networks due to cell-generated forces at the micron-scale. Fibroblasts were elongated-shaped in networks with ≤ 2 mg/ml fibrinogen, or cobblestone-shaped with 3 mg/ml fibrinogen at 24 h. At frequencies $f < 10^2$ Hz, G′ of fibroblast-seeded fibrin networks with ≥ 1 mg/ml fibrinogen increased compared to that of fibrin networks. At frequencies $f > 10^3$ Hz, G″ of fibrin networks decreased with increasing concentration following the power-law in frequency with exponents ranging from 0.75 ± 0.03 to 0.43 ± 0.03 at 3 h, and of fibroblast-seeded fibrin networks with exponents ranging from 0.56 ± 0.08 to 0.28 ± 0.06. In conclusion, fibroblasts actively contributed to a change in viscoelastic properties of fibrin networks at the micron-scale, suggesting that the cells and fibrin network mechanically interact. This provides better understanding of, e.g., cellular migration in wound healing.

Keywords One-particle microrheology · Microenvironment · Fibroblast · Fibrin · Mechanosensing · Viscoelasticity

Introduction

Fibrin is a resilient naturally occurring biopolymer and the main structural protein in blood clots, which stops bleeding, and promotes wound healing by serving as a provisional extracellular matrix for cells such as fibroblasts (Laurens et al. 2006; Jansen et al. 2013). Upon vascular injury, the enzyme thrombin converts the plasma protein fibrinogen in fibrin that can withstand forces exerted by flowing blood and by embedded cells (Kroll et al. 1996; Shah and Janmey 1997). Fibrin displays non-linear mechanical properties such as reversible strain-stiffening, whereby the material becomes stiffer as the stress or strain of the material increases, which protects fibrin to further deformation (Roberts et al. 1973; Janmey et al. 1983; Shah and Janmey 1997; Yao et al. 2008; Kang et al. 2009; Wen et al. 2012). Fibrin utilizes irreversible structural adaptations at multiple scales to maintain reversible stress stiffening up to large strains. It adapts to moderate strains at the network scale, whereas it adapts to high strains at the fiber scale. This multiscale self-adaptation mechanism provides fibrin the ability to cope with recurring loads due to shear flows and wound stretching (Kurniawan et al. 2016). A variety of tissue-forming cells such as fibroblasts can sense and respond to mechanical properties of their surrounding substrate by actively realigning and degrading the fibers, locally pulling on the fibers, and at the same time actively changing the stiffness and tension of the surrounding substrate by applying localized forces, so-called traction forces, in a mechanical-feedback loop (Wolf and Friedl 2011; Jansen et al. 2013). These changes in the surrounding substrate enable cells to sense mechanical signals over a distance of several cell lengths and can serve as a signal over a long range to neighboring cells to detect each other (Winer et al. 2009).

Jenneke Klein-Nulend and Rommel G. Bacabac contributed equally to this work.

✉ Jenneke Klein-Nulend
j.kleinnulend@acta.nl

[1] Department of Oral Cell Biology, Academic Centre for Dentistry Amsterdam (ACTA), University of Amsterdam and Vrije Universiteit Amsterdam, Amsterdam Movement Sciences, Gustav Mahlerlaan 3004, 1081 LA Amsterdam, The Netherlands

[2] Department of Dental Materials Science, Academic Centre for Dentistry Amsterdam (ACTA), University of Amsterdam and Vrije Universiteit Amsterdam, Amsterdam Movement Sciences, Amsterdam, The Netherlands

[3] Medical Biophysics Group, Department of Physics, University of San Carlos, Cebu City, Philippines

Characterization of mechanical properties at the micron-scale is difficult since both network and cell mechanics have complex underlying mechanisms. Rheology is used to measure the viscoelastic properties of fibrin networks using different rheological techniques (Ferry et al. 1997; Jansen et al. 2013; Kurniawan et al. 2016; Piechocka et al. 2016). Ferry et al. (1997) were the first to study the linear viscoelastic behavior of fibrin clots using torsional rheometry (Ferry et al. 1997). Thereafter, significant advances led to new applications of rheological techniques. Rheology has two main techniques, i.e., microrheology and macrorheology. Microrheology has advantages over macrorheology such as much smaller sample volume, a high-frequency bandwidth (0 to 100 kHz), in situ measurement, and higher sensitivity to intracellular dynamics (Mizuno et al. 2008; Tassieri et al. 2012). Microrheology can be classified as passive microrheology, measuring spontaneous thermally driven fluctuations of beads, or active microrheology, driving the beads by an external force (oscillatory optical tweezers or magnetic tweezers (Jones et al. 2015; Wessel et al. 2015)). Passive microrheology by using optical tweezers is non-invasive and can access the high-frequency domain, and can be used to characterize polymer network behavior (Morse 1998). Passive and active microrheology are suitable *to obtain information about the local micromechanical properties of extracellular matrix networks at the scale relevant to cells, as well as the network and fiber response* (Jansen et al. 2013).

Fibroblasts affect the macroscopic mechanical properties of fibrin (Winer et al. 2009), via active global stiffening of fibrin networks by applying traction forces (Jansen et al. 2013). The strain-stiffening response protects fibrin networks against damage from traction forces exerted by cells (Piechocka et al. 2016). While cell contractile activity is known to occur at the macro-scale, it is also important to know how cell contractile activity affects the local and global mechanical properties of the cell microenvironment and vice versa, the so-called mechanical-feedback loop. Since it is essential to elucidate this mechanical-feedback loop at the micron-scale for a better understanding of three-dimensional cell-matrix mechanical interactions, local matrix stiffness and cell-generated contractile stress are important parameters to study whether strain-stiffening can be induced on a cellular level. Therefore, we aimed to study the mechanical adaptation of fibrin networks due to cell-generated forces at the micron-scale. We hypothesized that fibrin networks adapt to cell-generated forces. We expected that cell-generated forces will increase the micromechanical properties of fibrin network. Fibrin networks and fibroblast-seeded fibrin networks were prepared with 1, 2, or 3 mg/ml fibrinogen polymerized with 0.5 IU/ml thrombin, and 1.0-μm polystyrene beads were embedded. Viscoelastic properties of fibrin networks and fibroblast-seeded fibrin networks were assessed 3 h after polymerization by one-particle passive optical tweezers microrheology.

Materials and methods

Cell culture

Human CCL-224 fibroblasts were cultured in T-75 culture flasks (Nunc, Roskilde, Denmark) in Dulbecco's modified Eagle medium (DMEM; Gibco, Paisley, UK) with 20% fetal bovine serum (FBS; Gibco, Paisley, UK) and 1% penicillin streptomycin (Gibco, Paisley, UK), and incubated at 37 °C in a humidified atmosphere with 5% CO_2. After 24 h, cells were cultured in DMEM with 10% FBS and 1% penicillin streptomycin, and the medium was refreshed every 3–4 days. Upon confluency, cells were harvested by incubation with 0.25% trypsin-ethylenediaminetetraacetic acid (EDTA; Gibco, Paisley, UK). Phosphate-buffered saline supplemented with 20% FBS was added to 0.25% trypsin-EDTA and to stop the trypsin-EDTA reaction, the cells were sequentially washed with phosphate-buffered saline to further remove the trypsin-EDTA, and no EDTA remnant was expected to have any impact on the clotting factor XIII activity. Fibroblasts were replated and cultured until passage 11 to be used in fibroblast-seeded fibrin networks to visualize the dynamics of cell spreading in fibrin networks.

Mouse L292 fibroblasts were cultured to near confluency in T-75 flasks in α-minimum essential medium (α-MEM; Gibco, Life Technologies, Waltham, MA, USA) with 10% FBS and 1% penicillin streptomycin. Fibroblasts were incubated at 37 °C in a humidified atmosphere with 5% CO_2, and subcultured until passage 3 to be used in fibroblast-seeded fibrin networks (see below) to perform one-particle passive microrheology.

Fibrin networks and fibroblast-seeded fibrin networks

Human fibrinogen powder (Enzyme Research, South Bend, IN, USA) was dissolved in a buffer of 20 mM sodium citrate-HCl, pH 7.4. For fibrin network preparation, fibrinogen solutions were mixed in fibrin assembly buffer containing 20 mM HEPES (Sigma-Aldrich, St. Louis, MO, USA), 150 mM NaCl, 5 mM $CaCl_2$ (pH 7.4), and 10% culture medium (89% α-MEM, 10% FBS, 1% penicillin streptomycin) for 10 min at 37 °C in a dry bath (Benchmark Scientific, Inc., Edison, NJ, USA). Fibrin networks were prepared with 1, 2, or 3 mg/ml fibrinogen with randomly embedded 1.0-μm-diameter polystyrene beads (Phosphorex, Hopkinton, MA, USA) and polymerized with 0.5 IU/ml human α-thrombin (Enzyme Research, South Bend, IN, USA) in a cell culture dish (diameter 35 mm; SPL Life Sciences Co., Ltd., Gyeonggi-do, Korea). Thirty minutes after the polymerization was initiated, fibrin networks were covered with culture medium and incubated at 37 °C in a humidified atmosphere with 5% CO_2 for 3 h.

Fibroblast-seeded fibrin networks were prepared by dissolving 1, 2, or 3 mg/ml human fibrinogen in fibrin assembly buffer (see above). Fibroblasts were resuspended in these three fibrinogen solutions with 1.0-μm-diameter polystyrene beads at a volume fraction of 10% and seeded at 500 cells/μl fibrinogen. Visual inspection by going from the bottom of the fibroblast-seeded fibrin networks to the top part by using a microscope revealed that the cell density was constant at different fibrinogen concentrations. Furthermore, the cell density was not suspected to vary dramatically within a few hours considering that the typical population doubling time of the human CCL-224 and mouse L292 fibroblasts takes 2 to 3 days. Fibroblast-seeded fibrinogen was polymerized with 0.5 IU/ml human α-thrombin in a cell culture dish. Thirty minutes after the polymerization was initiated, fibroblast-seeded fibrin networks were covered with culture medium and incubated at 37 °C in a humidified atmosphere with 5% CO_2 for 3 h.

For visualizing the dynamics of cell spreading in fibrin networks, fibroblast-seeded fibrin networks were imaged using a TCM400 inverted bright field microscope (LaboMed America, Inc., Fremont, CA, USA) immediately after seeding, and at 1, 2, and 24 h after cell seeding.

One-particle optical tweezers passive microrheology

One-particle passive microrheology was performed in steady-state conditions 3 h after polymerization (Jansen et al. 2013) with a customized optical tweezers microrheology setup (Fig. 2a). The motions of the embedded 1.0-μm-diameter polystyrene beads within fibrin and fibroblast-seeded fibrin networks covered with CO_2-independent medium (Gibco) in cell culture dishes were used for quantitative determination of the microscopic viscoelastic properties of fibrin and fibroblast-seeded fibrin networks with 1, 2, or 3 mg/ml fibrinogen. To demonstrate the cell-generated forces, one-particle passive microrheology was performed for 10-μm polystyrene beads embedded in 1, 2, or 3 mg/ml fibrin networks in cell culture dishes.

Polystyrene beads in the fibrin networks and fibroblast-seeded fibrin networks were weakly optically trapped using a ×100 objective (Zeiss, Thornwood, NY, USA) and a focused laser beam (MATRIX 1064-10-30, Coherent Inc., Santa Clara, CA, USA) with a wavelength of 1064 nm (Koenderink et al. 2006). The motions of the trapped beads were tracked by back-focal-plane interferometry. Thermally driven fluctuations of the micron-sized beads embedded in both types of fibrin networks were detected by a quadrant photodiode with a laser power of 15 mW at a sampling rate of 500 kHz and converted to the complex shear modulus G*, which is composed of the elastic modulus G′, and viscous modulus G″, to determine the viscoelastic properties by using the fluctuation-dissipation theorem (Gittes et al. 1997). The

power spectral density of the monitored bead is proportional to the imaginary component of the complex compliance, and by linear response theory, the real component of the complex compliance was calculated via a Kramers-Kronig integration. The complex shear modulus was then calculated as proportional to the inverse of the complex compliance via the generalized Stokes-Einstein relation (Gittes et al. 1997). As a control, one-particle optical tweezers passive microrheology was performed in water using the same micron-sized polystyrene beads.

Data analysis

A customized microrheology optical tweezers setup was used to determine the viscoelastic properties of unseeded and fibroblast-seeded fibrin networks. Spontaneous diffusive motions (thermal fluctuations) of 10 selected 1.0-μm beads, randomly embedded in fibrin and fibroblast-seeded fibrin networks, were measured per condition in the x and y direction at a fixed distance of 10 μm above the glass surface using customized LabVIEW software. The complex response function was determined by using the fluctuation-dissipation theorem to relate the bead motions to the thermal forces on the beads in the frequency domain (Mizuno et al. 2008). The viscoelastic properties as a function of frequency were obtained from the complex response function via the generalized Stokes-Einstein relation (Gittes et al. 1997; Mizuno et al. 2008). The data shown is the mean of five samples per condition calculated from a pool of 50 measurements of bead fluctuations, i.e., from 10 bead fluctuations per sample.

Results

Fibroblasts spread in fibrin networks

For visualizing the dynamics of cell spreading in fibrin networks, fibroblast-seeded fibrin networks were imaged with bright field microscopy immediately after seeding, and at 1, 2, and 24 h after cell seeding. Fibroblasts were round in all fibrin networks within 2 h after cell seeding, and spread in all fibrin networks after 24 h after cell seeding (Fig. 1). Twenty-four hours after cell seeding, cells were elongated in fibrin networks with 1 and 2 mg/ml fibrinogen, and had a cobblestone-shape in fibrin networks with 3 mg/ml fibrinogen (Fig. 1).

Mechanics of fibrin networks and fibroblast-seeded fibrin networks

The elastic modulus, G′, and viscous modulus, G″, of fibrin networks and fibroblast-seeded fibrin networks with different concentrations of fibrinogen were measured 3 h after
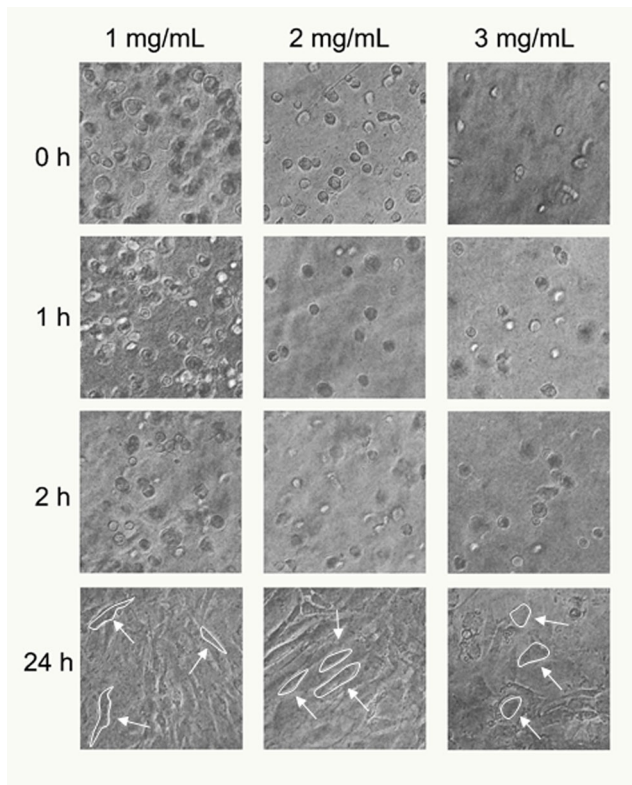
Fig. 1 Morphology of fibroblasts in fibrin networks containing 1, 2, or 3 mg/ml fibrinogen polymerized with 0.5 IU/ml thrombin immediately after seeding, and 1, 2, and 24 h after cell seeding. Cells were visualized by bright field microscopy. White arrows, cell boundary. Magnification × 20

polymerization by one-particle passive microrheology. In fibrin networks, the elastic modulus G′ (Fig. 2b) and the viscous modulus G″ (Fig. 2c) increased as the fibrinogen concentration increased from 1 to 3 mg/ml. Fibroblasts in all fibrin networks were still alive after performing one-particle passive microrheology. In fibroblast-seeded fibrin networks, at frequencies $f < 10^2$ Hz, the elastic modulus G′ increased as the fibrinogen concentration increased from 1 to 3 mg/ml (Fig. 3a). At frequencies $f > 10^4$ Hz, the viscous modulus G″ decreased as the fibrinogen concentration increased from 1 to 3 mg/ml (Fig. 3b). However, the G″ of fibroblast-seeded fibrin networks with 2 mg/ml (0.31 ± 0.05) was similar to that of fibroblast-seeded fibrin networks with 3 mg/ml (0.28 ± 0.06) (Fig. 3d). The elastic modulus of fibrin networks and fibroblast-seeded fibrin networks was higher in magnitude than the viscous modulus at frequencies $f < 10^2$ Hz (Figs. 2 and 4). Fibrin networks and fibroblast-seeded fibrin networks showed frequency-independent elastic moduli at frequencies $f < 10^2$ Hz (Fig. 3a), as well as fibrinogen concentration-dependent (Fig. 3c) elastic moduli at frequencies $f < 10^2$ Hz. At frequencies $f < 10^2$ Hz, G′ showed flattening, which reflects a local elastic plateau G_0 (Fig. 3a). For fibrin networks, G_0 increased with increasing fibrinogen concentration c following the power-law dependence $G_0 \approx c^{1.46 \pm 0.03}$ (Fig. 3c).

For fibroblast-seeded fibrin networks, G_0 increased with increasing fibrinogen concentration c following the power-law dependence $G_0 \approx c^{1.39 \pm 0.18}$ (Fig. 3c). The elastic modulus G′ of fibroblast-seeded fibrin networks with fibrinogen concentrations $c = 1$ mg/ml increased by 1.9-fold, $c = 2$ mg/ml increased by 2.0 fold, and $c = 3$ mg/ml increased by 1.6-fold compared to fibrin networks (Fig. 3a, c). G′ of fibrin networks embedded with 10-μm polystyrene beads was similar to fibrin networks for 1, 2, and 3 mg/ml fibrinogen (Fig. 4a–e). Fibrin networks and fibroblast-seeded fibrin networks showed frequency-dependent viscous moduli at frequencies $f > 10^3$ Hz (Fig. 3b) and fibrinogen-dependent (Fig. 3d) viscous moduli at frequencies $f > 10^3$ Hz. At frequencies $f > 10^3$ Hz, G″ of fibrin networks decreased with increasing concentration following the power-law dependence in frequency with $G″ \approx \omega^{0.75 \pm 0.03}$ for 1 mg/ml fibrinogen, $G″ \approx \omega^{0.50 \pm 0.07}$ for 2 mg/ml fibrinogen, and $G″ \approx \omega^{0.43 \pm 0.03}$ for 3 mg/ml fibrinogen (Fig. 3d). At frequencies $f > 10^3$ Hz, G″ of fibroblast-seeded fibrin networks decreased with increasing concentration following the power-law in frequency with $G″ \approx \omega^{0.56 \pm 0.08}$ for 1 mg/ml fibrinogen, $G″ \approx \omega^{0.31 \pm 0.05}$ for 2 mg/ml fibrinogen, and $G″ \approx \omega^{0.28 \pm 0.06}$ for 3 mg/ml fibrinogen (Fig. 3d). G″ of fibrin networks embedded with 10-μm polystyrene beads was similar to that of fibrin networks for 1, 2, and 3 mg/ml fibrinogen (Fig. 4b–f).

Discussion

We studied the mechanical adaptation of fibrin networks due to cell-generated forces at the micron-scale. We found that (i) fibroblasts were round in fibrin networks with 1, 2, and 3 mg/ml fibrinogen within 2 h after cell seeding, while 24 h after cell seeding, fibroblasts were elongated-shaped in fibrin networks with 1 and 2 mg/ml fibrinogen, and cobblestone-shaped in fibrin networks with 3 mg/ml fibrinogen; (ii) at frequencies $f < 10^2$ Hz, the elastic modulus G′ of fibroblast-seeded fibrin networks increased by 1.9-fold for 1 mg/ml fibrinogen, 2.0 fold for 2 mg/ml fibrinogen, and 1.6-fold for 3 mg/ml fibrinogen compared to fibrin networks; (iii) at frequencies $f > 10^3$ Hz, the viscous modulus G″ of fibrin networks decreased with increasing concentration following the power-law in frequency with exponents ranging from 0.75 ± 0.03 to 0.43 ± 0.03, while G″ of fibroblast-seeded fibrin networks decreased with increasing concentration following the power-law in frequency with exponents ranging from 0.56 ± 0.08 to 0.28 ± 0.06. Therefore, our results showed that fibroblasts generated forces causing microscopic matrix stiffening, suggesting that the cells and fibrin network mechanically interact. Fibroblasts were initially round in morphology, began to adhere to the fibrin fibers, and developed extensions as they changed from a round to an elongated-shaped or cobblestone-shaped phenotype 2 h after cell seeding. Cells embedded in fibrin networks

Fig. 2 Viscoelastic properties of fibrin networks with 1, 2, or 3 mg/ml fibrinogen polymerized with 0.5 IU/ml thrombin measured by one-particle passive microrheology 3 h after polymerization. **a** Schematic diagram of the customized optical tweezers microrheology setup. **b** Elastic moduli G′ of fibrin networks. **c** Viscous moduli G″ of fibrin networks. P, polarizer; M, mirrors; M3, steering mirror; BFP O, backfocal plane objective; DM, dichroic mirror; TL, telescope lens; QPD, quadrant photodiode; L, lens; BFP C, backfocal plane condenser; DIC, differential interference contrast microscopy; S, sample; LED, light emitting diode; CCD, charge-coupled device camera; PBS, polarizing beam splitter; AOD, acousto-optical device; BE, beam expander
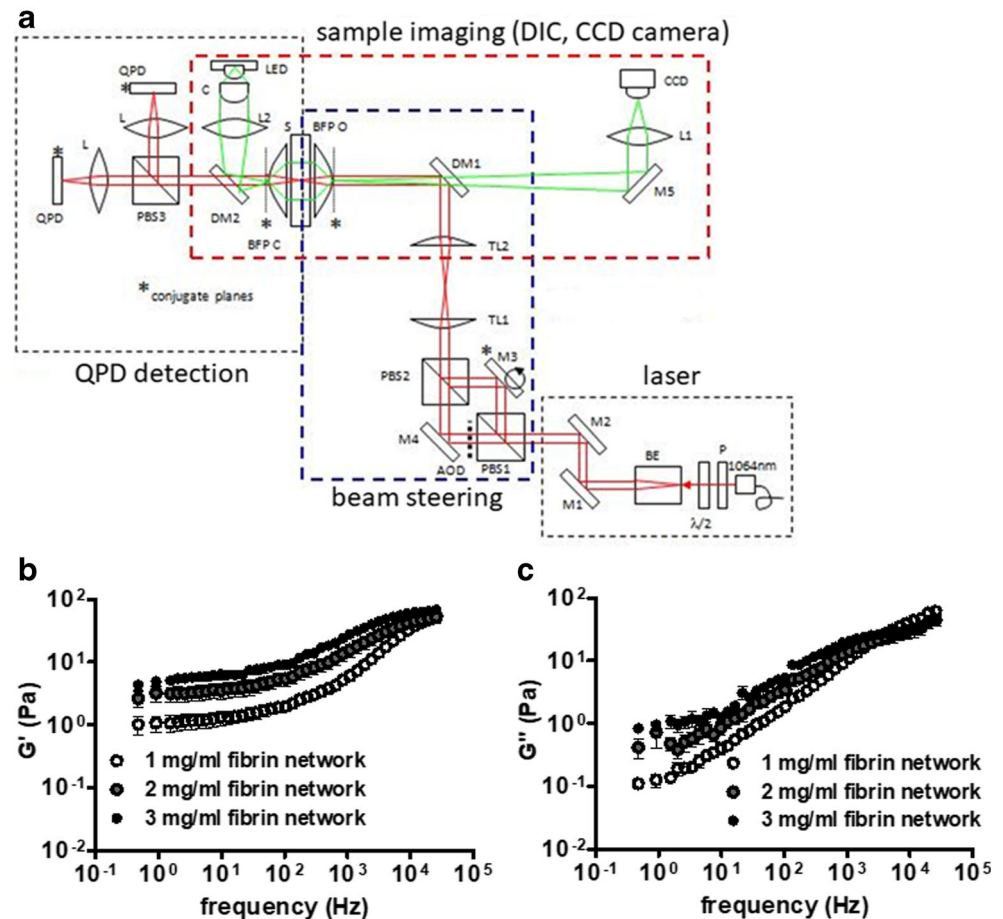
attach and exert traction forces on the fibers of the surrounding network (Notbohm et al. 2015). These forces lead to reorganization of the matrix fibers around them (Notbohm et al. 2015). Reorganization is the first stage of the matrix remodeling process and takes place over a few hours to a few days (Piechocka et al. 2010). Structural remodeling of fibrin networks due to cellular traction forces is a complex process, in part because fibrin networks are not linearly elastic, exhibiting strain-stiffening when subjected to large deformations (Piechocka et al. 2010). The differences found in cellular shape between the dilute fibrin networks with 1 or 2 mg/ml fibrinogen and the denser fibrin network with 3 mg/ml fibrinogen 1 day after cell seeding indicate differences in reorganization. Fibroblasts change cellular shape most pronounced in dilute fibrin networks with fibrinogen concentrations $c \leq 2$ mg/ml compared to denser fibrin networks with fibrinogen concentrations $3 \leq c \leq 6$ mg/ml (Jansen et al. 2013). Cells in dilute fibrin networks are elongated and extend several thin protrusions into the network, while cells in denser fibrin networks remain round and extend short and thin protrusions into the network (Jansen et al. 2013). Since mesh size decreases with the square-root of fibrinogen concentration (Piechocka et al. 2010), the smaller mesh size in dense fibrin networks can constrain the cell body and can impede the extensions of

protrusions. Fibrin's plasticity can direct and control cell morphology and migration (Notbohm et al. 2015). Plastic deformation of fibrin networks leaves tube-like matrix gaps with available space for subsequent growth of cell extension (Notbohm et al. 2015). Another explanation for the differences in cellular shape can be that the dilute fibrin networks are more plastically deformed than the denser fibrin networks, suggesting more available space for cell protrusions. Thus, the structure of the microenvironment around cells in dilute fibrin networks differs from dense fibrin networks, which might lead to altered mechanical properties of the microenvironment. In previous unpublished work, fibroblasts destroyed the fibrin network, possibly by proteolytic activity, after a period of about 16 h in culture. This was visually confirmed by observing large "hole" structures in the fibrin network close to the cells. Since the current study addresses the micromechanical properties of fibrin networks and fibroblast-seeded fibrin networks 3 h after polymerization, further studies are needed to correlate the onset of cell spreading and the onset of gel-stiffening and plasticity. Furthermore, rheology measurements should be performed within a time period much lower than 24 h at which time it is suspected that the fibrin network would not resemble homogeneous and intact structure anymore.
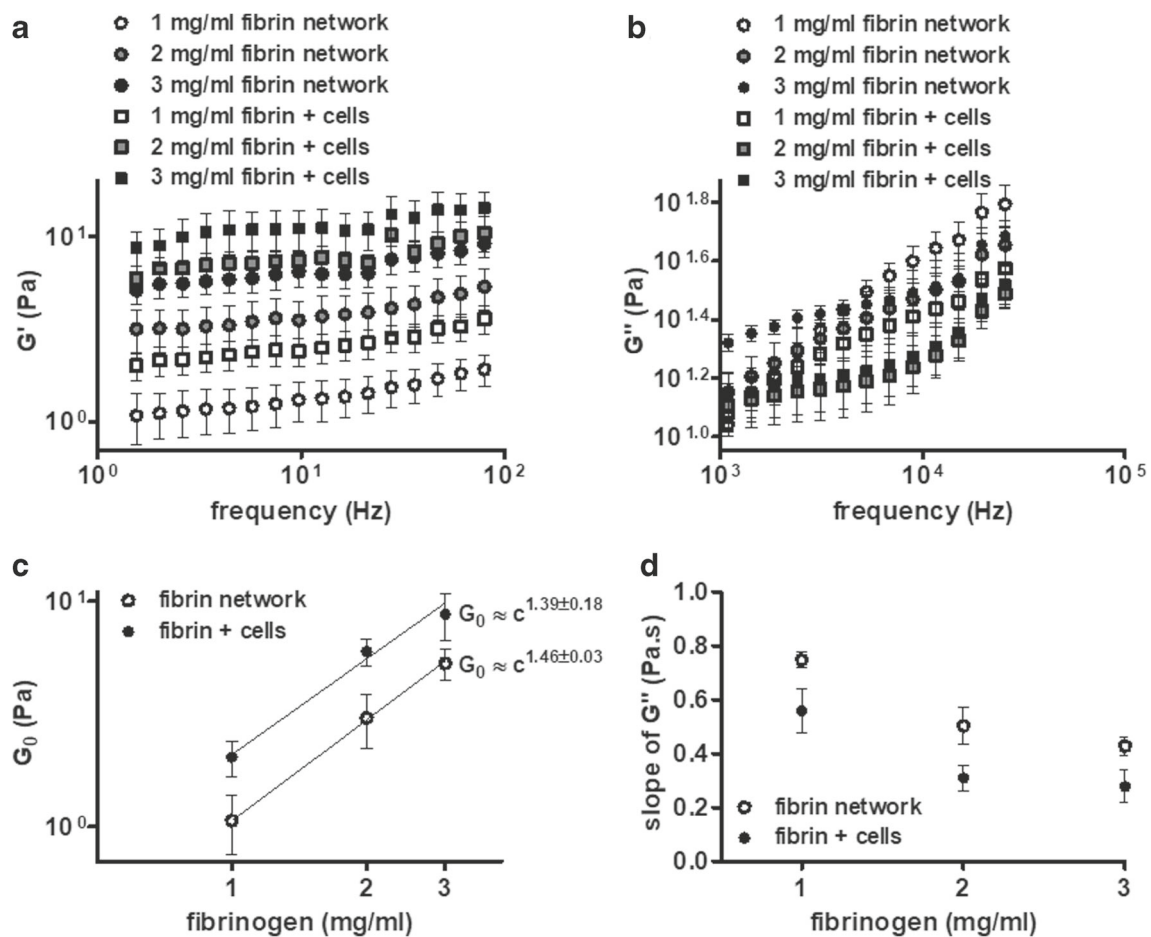
Fig. 3 Viscoelastic properties of fibrin networks and fibroblast-seeded fibrin networks with 1, 2, and 3 mg/ml fibrinogen polymerized with 0.5 IU/ml thrombin measured by one-particle passive microrheology 3 h after polymerization. **a** Elastic moduli G′ of fibrin networks and fibroblast-seeded fibrin networks at frequencies $f < 10^2$ Hz. **b** Viscous moduli G″ of fibrin networks and fibroblast-seeded fibrin networks at frequencies $f > 10^3$ Hz. **c** Elastic plateau G_0 of fibrin networks and fibroblast-seeded fibrin networks at frequencies $f < 10^2$ Hz. **d** Slope of viscous moduli G″ of fibrin networks and fibroblast-seeded fibrin networks at frequencies $f > 10^3$ Hz

The elastic modulus in the elastic plateau region G_0 of semiflexible polymers follows a power-law in concentration with an exponent of 11/5 (MacKintosh et al. 1995; Gardel et al. 2004). In our study, G_0 of fibrin networks followed a power-law in concentration with an exponent of 1.5. This exponent is in good agreement with prior measurements on fibrin networks where G_0 followed a power-law in concentration with an exponent of nearly 2.0 and 2.3 measured by macrorheology (Jansen et al. 2013; Piechocka et al. 2010). The magnitude of the moduli measured by macrorheology is greater than our measurement. Fibrin networks were prepared under similar fibrin conditions, but in our study, the fibrinogen concentration range was small, i.e., 1 to 3 mg/ml, compared to other studies where the range was 0.1 to 6 mg/ml (Jansen et al. 2013) and 0.1 to 8 mg/ml (Piechocka et al. 2010). The difference in magnitude of the moduli can be explained by the smaller range of fibrinogen concentration used in our study.

The elastic modulus of fibroblast-seeded fibrin networks was 1.6–2.0-fold higher than that of fibrin networks at frequencies $f < 10^2$ Hz for all fibrinogen concentration. Prior macrorheology measurements on fibrin networks with and without fibroblasts show a threefold higher G′ for fibroblast-seeded fibrin networks for $c \leq 2$ mg/ml, but for fibrinogen concentrations $c > 2$ mg/ml, the cells do not significantly influence the elastic modulus (Jansen et al. 2013). The difference we observed in G′ between fibroblast-seeded fibrin networks and fibrin networks might be due to higher local traction forces at higher fibrin concentrations corresponding to an increase in elastic modulus at the micron-scale, but not at the macroscopic scale. Microrheology measurements showed that cells stiffened the fibrin networks starting 3 h after cell seeding for higher fibrinogen concentrations.

The viscous modulus G″ of semiflexible networks follows a power-law in frequency with exponent ¾ (Gittes and MacKintosh 1998). In our study, the probable exponential decrease in the exponents of the G″ could be related to the stiffening of fibrin as well as the decrease in mesh size with increasing fibrinogen concentration. The same result was

Fig. 4 Viscoelastic properties of fibrin networks with 1.0- or 10-μm-diameter polystyrene beads and fibroblast-seeded fibrin networks with 1.0-μm-diameter polystyrene beads with 1, 2, and 3 mg/ml fibrinogen polymerized with 0.5 IU/ml thrombin measured by one-particle passive microrheology 3 h after polymerization. **a, b** Fibrin networks with 1.0- or 10-μm-diameter polystyrene beads and fibroblast-seeded fibrin networks with 1.0-μm diameter polystyrene beads with 1 mg/ml fibrinogen. **c, d** Fibrin networks with 1.0- or 10-μm-diameter polystyrene beads and fibroblast-seeded fibrin networks with 1.0-μm-diameter polystyrene beads with 2 mg/ml fibrinogen. **e, f** Fibrin networks with 1.0- or 10-μm-diameter polystyrene beads and fibroblast-seeded fibrin networks with 1.0-μm-diameter polystyrene beads with 3 mg/ml fibrinogen. **a, c, e** Elastic moduli G′ of fibrin networks and fibroblast-seeded fibrin networks. **b, d, f** Viscous moduli G″ of fibrin networks and fibroblast-seeded fibrin networks
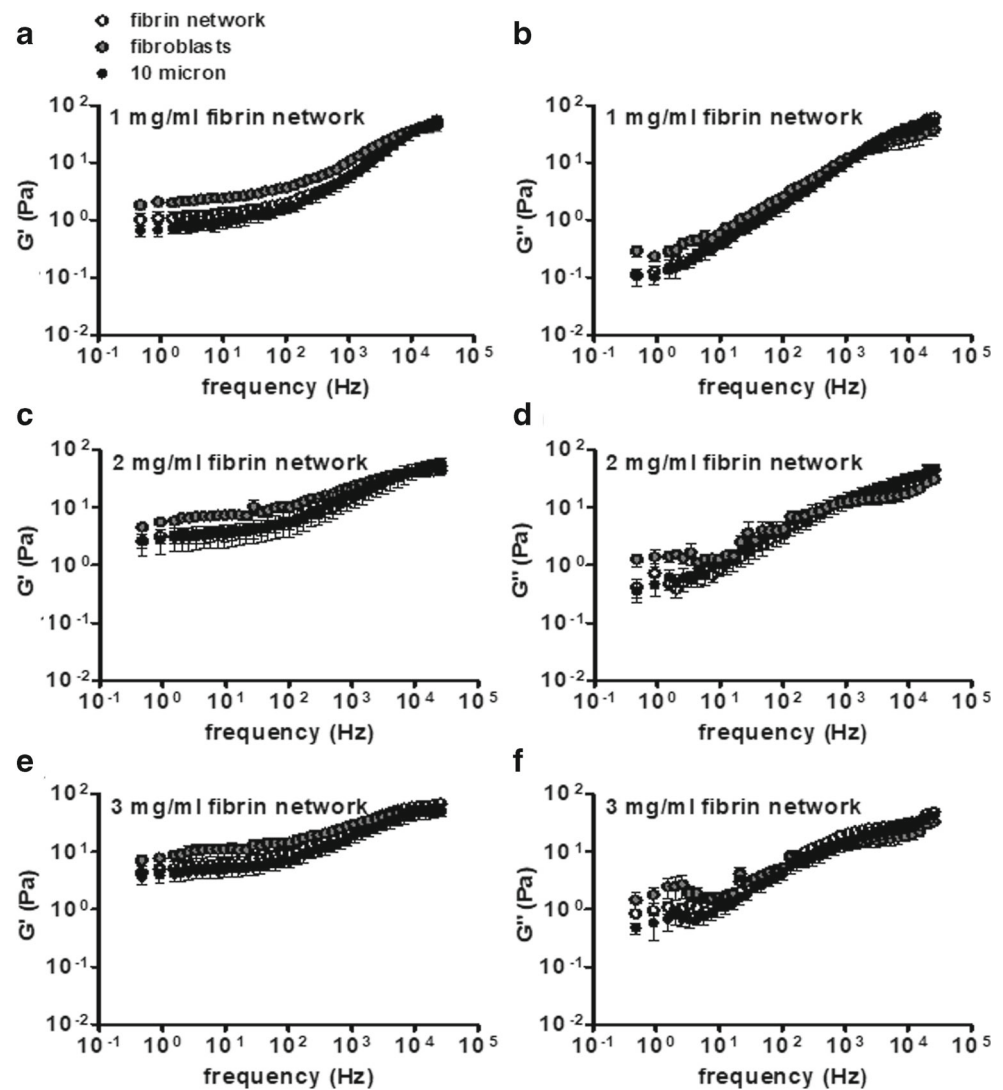
found for fibroblast-seeded fibrin networks where the exponents decreased with increasing fibrinogen concentration. This might indicate that cells do not constrain the formation of a uniform fibrin network, which results in a lower viscous network.

To unravel the mechanical-feedback loop between cell contractile activity and the local and global mechanical properties of their microenvironment, it is also important to take the ability of cells to push against the matrix as well as the nucleus into account. The nucleus also exhibits viscoelastic properties (Guilak et al. 2000). It is tightly coupled to the surrounding cytoskeleton, which in turn is physically connected to the extracellular matrix. Deformations of the nucleus can have important consequences for cellular functions, such as gene expression, resulting in defective nuclear cytoskeletal coupling and defects in cytoskeletal organization and stiffness, thereby affecting tissue function. Cells align fibrin fibers by pulling on the surrounding matrix, and compact fibrin fibers by pushing against the matrix, to invade the matrix and create

permanent deformation of the matrix (Notbohm et al. 2015). The magnitude of pulling and pushing forces is roughly of the same order, but the location of these forces in the matrix changes over time (Notbohm et al. 2015). Pulling forces appear along the leading edges of cellular protrusions, whereas pushing forces often appear near the cell body and vary with time near the tip of a growing cell protrusion (Notbohm et al. 2015). This indicates that compressive forces are present within the cell which might be the result of nuclear deformation. Future studies are needed to investigate the mechanism underlying how cells push against the matrix.

In summary, cellular shape is both fibrinogen concentration- and time-dependent. The incorporation of fibroblasts into fibrin networks increases the elastic moduli and decreases the viscous moduli of fibrin networks, which might drive the fibrin networks into a non-linear stress-stiffened state. Therefore, our results show that the presence of fibroblasts in fibrin networks actively contribute to a change in viscoelastic properties of fibrin networks at the micron-scale,

suggesting that the cells and fibrin network mechanically interact. This contributes to a better understanding of biologically relevant processes, such as cellular migration in infection, inflammation, immunology, and wound healing.

Publisher's Note Springer Nature remains neutral with regard to jurisdictional claims in published maps and institutional affiliations.

References

Ferry B, Antrobus P, Huzicka I, Farrell A, Lane A, Chapel H (1997) Intracellular cytokine expression in whole blood preparations from normals and patients with atopic dermatitis. Clin Exp Immunol 110: 410–417. https://doi.org/10.1046/j.1365-2249.1997.4361452.x

Gardel ML, Shin JH, MacKintosh FC, Mahadevan L, Matsudaira P, Weitz DA (2004) Elastic behavior of cross-linked and bundled actin networks. Science 304:1301–1305. https://doi.org/10.1126/science.1095087

Gittes F, MacKintosh FC (1998) Dynamic shear modulus of a semiflexible polymer network. Phys Rev E 58:R1241–R1244. https://doi.org/10.1103/PhysRevE.58.R1241

Gittes F, Schnurr B, Olmsted PD, MacKintosh FC, Schmidt CF (1997) Microscopic viscoelasticity: shear moduli of soft materials determined from thermal fluctuations. Phys Rev Lett 79:3286–3289. https://doi.org/10.1103/PhysRevLett.79.3286

Guilak F, Tedrow JR, Burgkart R (2000) Viscoelastic properties of the cell nucleus. Biochem Biophys Res Commun 269:781–786. https://doi.org/10.1006/bbrc.2000.2360

Janmey PA, Amis EJ, Ferry JD (1983) Rheology of fibrin clots. VI. Stress relaxation, creep, and differential dynamic modulus of fine clots in large shearing deformations. J Rheol 27:135–153. https://doi.org/10.1122/1.549722

Jansen KA, Bacabac RG, Piechoka IK, Koenderink GH (2013) Cells actively stiffen fibrin networks by generating contractile stress. Biophys J 105:2240–2251. https://doi.org/10.1016/j.bpj.2013.10.008

Jones CAR, Cibula M, Feng J, Krnacik EA, McIntyre DH, Levine H, Sun B (2015) Micromechanics of cellularized biopolymer networks. Proc Natl Acad Sci U S A 112:E5117–E5122. https://doi.org/10.1073/pnas.1509663112

Kang H, Wen Q, Janmey PA (2009) Non-linear elasticity of stiff filament networks: strain stiffening, negative normal stress, and filament

alignment in fibrin gels. J Phys Chem B 26:3799–3805. https://doi.org/10.1021/jp807749f

Koenderink GH, Atakhorrami M, MacKintosh FC, Schmidt CF (2006) High-frequency stress relaxation in semiflexible polymer solutions and networks. Phys Rev Lett 96:138307. https://doi.org/10.1103/PhysRevLett.96.138307

Kroll MH, Hellums JD, McIntire LV, Schafer AI, Moake JL (1996) Platelets and shear stress. Blood 88:1525–1541

Kurniawan NA, Vos BE, Biebricher A, Wuite GJL, Peterman EJG, Koenderink GH (2016) Fibrin networks support recurring mechanical loads by adapting their structure across multiple scales. Biophys J 111:1026–1034. https://doi.org/10.1016/j.bpj.2016.06.034

Laurens N, Koolwijk P, de Maat MPM (2006) Fibrin structure and wound healing. J Thromb Haemost 4:932–939. https://doi.org/10.1111/j.1538-7836.2006.01861.x

MacKintosh FC, Käs J, Janmey PA (1995) Elasticity of semiflexible biopolymer networks. Phys Rev Lett 75:4425–4428. https://doi.org/10.1103/PhysRevLett.75.4425

Mizuno D, Head DA, MacKintosh FC, Schmidt CF (2008) Active and passive microrheology in equilibrium and nonequilibrium systems. Macromolecules 41:7194–7202. https://doi.org/10.1021/ma801218z

Morse DC (1998) Viscoelasticity of tightly entangled solutions of semiflexible polymers. Phys Rev E 58:R1237–R1240. https://doi.org/10.1103/PhysRevE.58.R1237

Notbohm J, Lesman A, Tirrell DA, Ravichandran G (2015) Quantifying cell-induced matrix deformation in three dimensions based on imaging matrix fibers. Integr Biol 7:1186–1195. https://doi.org/10.1039/C5IB00013K

Piechocka IK, Bacabac RG, Potters M, MacKintosh FC, Koenderink GH (2010) Structural hierarchy governs fibrin gel mechanics. Biophys J 98:2281–2289. https://doi.org/10.1016/j.bpj.2010.01.040

Piechocka IK, Jansen KA, Broedersz CP, Kurniawan NA, MacKintosh FC, Koenderink GH (2016) Multi-scale strain-stiffening of semiflexible bundle networks. Soft Matter 12:2145–2156. https://doi.org/10.1039/C5SM01992C

Roberts WW, Lorand L, Mockros LF (1973) Viscoelastic properties of fibrin clots. Biorheology 10:29–42

Shah JV, Janmey PA (1997) Strain hardening of fibrin gels and plasma clots. Rheol Acta 36:262–268. https://doi.org/10.1007/BF00366667

Tassieri M, Evans RML, Warren RL, Bailey NJ, Cooper JM (2012) Microrheology with optical tweezers: data analysis. New J Phys 14:115032. https://doi.org/10.1088/1367-2630/14/11/115032

Wen Q, Basu A, Janmey PA, Yodh AG (2012) Non-affine deformations in polymer hydrogels. Soft Matter 8:8039–8049. https://doi.org/10.1039/c2sm25364j

Wessel AD, Gumalla M, Grosshans J, Schmidt CF (2015) The mechanical properties of early drosophila embryos measured by high-speed video microrheology. Biophys J 108:1899–1907. https://doi.org/10.1016/j.bpj.2015.02.032

Winer JP, Oake S, Janmey PA (2009) Non-linear elasticity of extracellular matrices enables contractile cells to communicate local position and orientation. PLoS One 4:e6382. https://doi.org/10.1371/journal.pone.0006382

Wolf K, Friedl P (2011) Extracellular matrix determinants of proteolytic and non-proteolytic cell migration. Trends Cell Biol 21:736–744. https://doi.org/10.1016/j.tcb.2011.09.006

Yao NY, Larsen RJ, Weitz DA (2008) Probing nonlinear rheology with inertio-elastic oscillations. J Rheol 52:1013–1025. https://doi.org/10.1122/1.2933171